



Published in final edited form as:

*J Pain*. 2013 October ; 14(10): 1031–1044. doi:10.1016/j.jpain.2013.03.012.

## Induction of monocyte chemoattractant protein-1 (MCP-1) and its receptor CCR2 in primary sensory neurons contributes to paclitaxel-induced peripheral neuropathy

Haijun Zhang<sup>1</sup>, Jessica A. Boyette-Davis<sup>1,†</sup>, Alyssa K. Kosturakis<sup>1</sup>, Yan Li<sup>1</sup>, Seo-Yeon Yoon<sup>1,†</sup>, Edgar T. Walters<sup>2</sup>, and Patrick M. Dougherty<sup>1</sup>

<sup>1</sup>The Department of Anesthesia and Pain Medicine Research, The University of Texas M.D. Anderson Cancer Center, Houston, Texas 77030

<sup>2</sup>The Department of Integrative Biology and Pharmacology, The University of Texas Health Science Center at Houston, Houston, Texas 77030

### Abstract

The use of paclitaxel (Taxol®), a microtubule stabilizer, for cancer treatment is often limited by its associated peripheral neuropathy (chemotherapy-induced peripheral neuropathy, CIPN) which predominantly results in sensory dysfunction including chronic pain. Here we show that paclitaxel CIPN was associated with an induction of chemokine monocyte chemoattractant protein-1 (MCP-1) and its cognate receptor CCR2 in primary sensory neurons of dorsal root ganglia (DRG). Immunostaining revealed that MCP-1 was mainly expressed in small nociceptive neurons while CCR2 was expressed in large and medium-sized myelinated neurons. Direct application of MCP-1 consistently induced intracellular calcium increases in DRG large and medium-sized but not small neurons mainly dissociated from paclitaxel- but not vehicle-treated animals. Paclitaxel also induced increased expression of MCP-1 in spinal astrocytes but no CCR2 signal was detected in spinal cord. Local blockade of MCP-1/CCR2 signaling by anti-MCP-1 antibody or CCR2 antisense oligodeoxynucleotides significantly attenuated paclitaxel CIPN phenotypes including mechanical hypersensitivity and loss of intraepidermal nerve fibers (IENFs) in hindpaw glabrous skin. These results suggest that activation of paracrine MCP-1/CCR2 signaling between DRG neurons plays a critical role in the development of paclitaxel CIPN and targeting MCP-1/CCR2 signaling could be a novel therapeutic approach.

### Keywords

Paclitaxel; neuropathy; DRG; MCP-1; CCR2

---

© 2013 The American Pain Society. Published by Elsevier Inc. All rights reserved.

Corresponding Authors: Haijun Zhang, MD, Department of Pain Medicine, The University of Texas M.D. Anderson Cancer Center, 1515 Holcombe Blvd. U110, Y6.5710, Houston, TX 77030, Tel: 713-745-3045, Fax: 713-794-4590, haijun.zhang@mdanderson.org.  
†current address: The Department of Psychology, York College, York, Pennsylvania (J.B.D.); The laboratory of Molecular Signal Transduction, Center for Neural Science, Korea Institute of Science and Technology, Seoul, South Korea (S.Y.Y.).

This is a PDF file of an unedited manuscript that has been accepted for publication. As a service to our customers we are providing this early version of the manuscript. The manuscript will undergo copyediting, typesetting, and review of the resulting proof before it is published in its final citable form. Please note that during the production process errors may be discovered which could affect the content, and all legal disclaimers that apply to the journal pertain.

### DISCLOSURES

The authors declare no conflict of interest.

## INTRODUCTION

Chemotherapy-induced peripheral neuropathy (CIPN) is a very common side effect of several frontline chemotherapeutic drugs including paclitaxel, oxaliplatin and bortezomib<sup>15</sup>. CIPN usually presents as a pronounced impairment in sensory function in a glove-and-stocking distribution in glabrous skin but with relative sparing of motor and autonomic functions<sup>37,41</sup>. Although CIPN following paclitaxel has been considered as a polyneuropathy, the incidence of symptoms of numbness and tingling is more prominent than the experience of shooting/burning pain<sup>21,41</sup>, suggesting a greater impairment of large (A) and medium-sized (A) myelinated fiber function than of unmyelinated (C) fiber function<sup>21</sup>.

The mechanisms of CIPN are not well understood and the treatment is not satisfactory. It has been assumed though without direct evidence that the neuropathy associated with paclitaxel is due to effects on axonal microtubules, which results in interruption of axoplasmic flow and subsequently damages peripheral nerves<sup>58,68</sup>. However changes in axonal architecture were not apparent in rats with taxol-induced hyperalgesia<sup>51</sup> and axonal transport was not impaired in dorsal root ganglia (DRG) neurons exposed to paclitaxel *in vitro* at chemotherapeutic doses<sup>28</sup>. Reagents that disrupt the functions of microtubules such as TZT-1027 (a derivative of dolastatin) or colchicine<sup>4,17</sup> do not induce any morphological change in sensory nerves or hyperalgesia<sup>47,73</sup>. Although direct application of colchicine to the sciatic nerve blocks neurogenic plasma extravasation, changes of heat or mechanical withdrawal thresholds or the development of deafferentation-induced hyperalgesia have not been observed<sup>33</sup>.

Cytokine-mediated neuroinflammation has been suggested to play a critical role in the pathogenesis of neuropathic pain not only after nerve injury (for review, see<sup>44</sup>) but also in CIPN<sup>67</sup>. Recently, chemokines (chemotactic cytokines) which attract the migration of leukocytes associated with inflammation have been shown to be involved in the initiation of neuropathic pain<sup>69</sup>. Several types of chemokines and their receptors are markedly induced in the nervous system following experimental peripheral neuropathy<sup>7,8</sup>. Of those many chemokines, monocyte chemoattractant protein-1 (MCP-1), also CCL2, has been found universally increased in the nervous system in different models of neuropathic pain<sup>35</sup> including compression of dorsal root ganglion (DRG)<sup>70</sup> and peripheral nerve injury<sup>1,7,9,23,25,30,63,64,76,78</sup>. In addition, attenuation of neuropathic pain following nerve injury is observed by blocking MCP-1 and/or its cognate receptor CCR2<sup>7,9,23,25,64,66,78</sup> as well as in CCR2 knockout mice<sup>1</sup>. It has been further shown that direct application of MCP-1 excites C-fibers following neuritis<sup>54</sup>, increases the excitability of DRG neurons following injury<sup>62,70</sup>, induces increases in intracellular calcium in DRG neurons<sup>7,9</sup>, and increases capsaicin-induced currents<sup>31</sup> and tetrodotoxin-resistant sodium currents of peripheral nociceptors<sup>6</sup>. It is not known if MCP-1/CCR2 signaling is involved in the development of CIPN. In the present study, we examined the expression of MCP-1 and CCR2 in both DRG and spinal dorsal horn (SDH) using a rat model of paclitaxel CIPN and the effects of blocking MCP-1/CCR2 signaling on the paclitaxel CIPN phenotypes.

## MATERIALS AND METHODS

### Animals

Adult male Sprague-Dawley rats (6–12 weeks, Harlan, Houston, TX, USA) housed in a 12 h light/dark cycle with free access to food and water were used in all experiments. The studies were approved by the Institutional Animal Care and Use Committee at The University of Texas M. D. Anderson Cancer Center and were performed in accordance with the National Institutes of Health Guidelines for Use and Care of Laboratory Animals.

### Paclitaxel CIPN model

Animals were treated with paclitaxel as previously described<sup>11</sup>. Briefly, paclitaxel stock solution (6 mg/ml, dissolved in cremophor EL/ethanol, TEVA Pharmaceuticals, Inc. USA) was diluted with sterile 0.9% saline to 1 mg/ml and given at a dosage of 2 mg/kg (intraperitoneally) every other day for a total of four injections (Day 1, 3, 5, and 7). This dosage is equal to ~ 15 mg/m<sup>2</sup> which is roughly 1/10 of the chemotherapy dosage used in humans (~ 175 mg/m<sup>2</sup>). Control animals received an equivalent volume of vehicle (cremophor EL/ethanol 1:1) (see Fig. 5A for treatment regimen). Rats were observed carefully for any abnormal behavioral changes twice a week following the treatment. Clear-cut signs of peripheral neuropathy with a similar phenotype as in patients have been validated in this non-tumor-bearing animal model of paclitaxel CIPN by multiple investigators<sup>11,14,20,51</sup>.

### Intrathecal treatment

Intrathecal drug delivery was performed by lumbar puncture as previously described<sup>18,72</sup>. Rats were anesthetized with isoflurane (2.5%) and injected in the L5-L6 intervertebral space using a 0.5-inch 30-gauge needle connected to a luer-tipped Hamilton syringe. Correct subarachnoid positioning of the tip of the needle was verified by tail-flick. Anti-MCP-1 IgG (500 µg/ml, 10 µl per application, R&D)<sup>64</sup> or equal amount of nonspecific IgG (NS IgG) was delivered intrathecally 24 hours prior to the first injection of paclitaxel and was continued once daily for the next 7 days for a total of 8 injections (Day 0–7). On days when both drugs were administered, intrathecal treatment was given 30 minutes prior to paclitaxel. Rats were monitored for an additional 10 minutes after injection. The knockdown of CCR2 in DRG was achieved by intrathecal delivery of antisense oligodeoxynucleotides (ODNs) which has been shown to transiently inhibit the expression of various proteins in DRG in many studies<sup>2,10,36</sup>. The antisense ODN sequence 5'-ACTCGGTCTGCTGTCTCCCTA-3' (Invitrogen) was directed against a unique sequence of the rat CCR2 gene (GenBank number NM021866) while the mismatch sequence (as control) included six substituted bases (indicated in bold face, 5'-ACACGCTGTCCTGTC**AG**CCTA-3'). The lyophilized ODNs were reconstituted in nuclease-free ultrapure water to a concentration of 8 µg/µl and stored at -20°C until use. A total of 40 µg antisense or mismatch ODNs diluted with 0.9% saline was delivered once daily for four injections starting at 14 days following chemotherapy (Day 14–17).

### Mechanical threshold

Mechanical sensitivity was assessed by determination of the 50% withdrawal threshold to von Frey filament stimulation applied to the mid-plantar surface of the hind paw described previously<sup>11</sup>. Briefly, the testing session began by applying the lowest force monofilament to the left and then right hindpaw for approximately 1 second, followed by the next higher force monofilament. To test the mechanical threshold after the delivery of anti-MCP-1 neutralizing antibody, each filament was repeated 6 times for each paw. The 50% threshold was determined by the monofilament at which the animal made a response of paw withdrawal, flinching, or licking 6 out of the 12 applications. Animals receiving CCR2 antisense or mismatch ODNs treatment were assessed by the “up-and-down” method according to Chaplan et al<sup>16</sup>. The testers were blinded to treatment conditions.

### Quantitative real-time polymerase chain reaction (qRT-PCR)

Homogenates of L4/L5 DRGs and lumbar SDH (L4-L6, dorsal half of spinal cord including the associated white matter) tissue for qRT-PCR were prepared as previously described. Total RNA was extracted using TRIzol Reagent (Invitrogen, Carlsbad, CA, USA) and complementary DNA (cDNA) from 1µg of total RNA was performed using Superscript III

First-Strand Synthesis SuperMix (Invitrogen). The amplification of cDNA was performed using SYBR Green PCR Master Mix (ABI, Warrington, UK) with the following primers: CCR2 (NM02866): 5'-AGGGGGCCACCACACCGTATGA-3' (F), 5'-CATGTTGCCACAAAACCAAAGATGAA-3' (R); glyceraldehyde-3-phosphate-dihydrogenase (GAPDH, NM01008): 5'-TGCCAAGTATGATGACATCAAGAAG-3' (F), 5'-AGCCCAGGATGCCCTTTAGT-3' (R). Amplification steps consisted of one cycle of 50°C for 2 minutes plus 95°C for 10 minutes, 40 cycles of 95°C for 15 seconds, 55°C for 25 seconds and 72°C for 1 minute, and one cycle of 95°C for 15 seconds, 60°C for 20 seconds and 95°C for 15 seconds as a dissociation stage. The threshold cycle ( $C_t$ ; the number of cycles to reach the threshold of detection) was determined for each gene and the relative expression level of each gene was calculated using the following formula: relative expression of mRNA =  $2^{-(C_{t_{\text{sample}}} - C_{t_{\text{control}}})}$ , where  $C_{t_{\text{sample}}}$  is the  $C_t$  for the target gene and  $C_{t_{\text{control}}}$  is the  $C_t$  for the housekeeping gene GAPDH<sup>59</sup>.

### Immunohistochemistry

Animals were deeply anesthetized with sodium pentobarbital (Nembutal, 100 mg/kg, i.p.), transcardially perfused with warm saline followed by cold 4% paraformaldehyde or Zamboni's fixative. Spinal cord and DRGs (L4, L5, C7, T5 and T6) were removed and postfixed overnight in the same solution and then cryoprotected in 30% sucrose solution at 4°C. Sections of DRG (20 µm) and lumbar spinal cord (L4-L6, transverse, 25 µm) were made in a cryostat and processed for immunofluorescent staining. Every fourth section from each sample was collected to probe the same protein. Sections were first blocked with 10% normal donkey serum (NDS) and 0.2% Triton X-100 in PBS for 1 hr at room temperature and then incubated overnight at 4°C in 5% NDS and 0.2% Triton X-100 in PBS containing the following primary antibodies: MCP-1 (rabbit, 1:500, Millipore); CCR2 (goat, 1:500, Santa Cruz); NF200 (mouse, 1:2000, Sigma); TRPV1 (goat, 1:1000, Neuromics); CGRP (guinea pig, 1:2000, Peninsula Labs); GFAP (mouse, 1:1000, Cell Signaling Technology), OX-42 (mouse, 1:1000, Serotec), NeuN (mouse, 1:1000, Millipore). For double staining, two antibodies from different species will be mixed and incubated with sections. After washing, the sections were then incubated with Cy3- or FITC-conjugated secondary antibodies (Jackson ImmunoResearch) overnight at 4°C. Some experiments were augmented with the addition of *Bandeiraea (griffonia) simplicifolia* I-isolectin B4 (IB4) conjugated with FITC (L2895, Sigma). Sections were then mounted and viewed under a confocal microscope (Nikon A1, Nikon, Japan). The antibody to MCP-1 has been used and verified by other studies<sup>7,9</sup>. To verify the specificity of anti-CCR2 antibody, pre-absorption experiment was done by incubating antibody with CCR2 protein (1:200, Santa Cruz) followed by the regular immunohistochemical steps.

Immunohistochemical staining of skin was performed as previously described<sup>11</sup>. One 3-mm skin biopsy was taken from each hindpaw from animals on Day 28 following chemotherapy. Every third skin section (25 µm) was collected to probe protein gene product 9.5 (PGP9.5, rabbit; 1:1000, AbD Serotec) and collagen IV (goat; 1:250, Southern Biotech). PGP9.5 reliably immunostains IENFs and collagen IV stains the basement membrane at the dermal/epidermal junction.

### Quantification

All quantifications were made with NIC Elements imaging software (Nikon, Japan) from images previously captured and digitally stored. For a given experiment, all images were taken using identical acquisition parameters and the final representative figures are presented as the original images without further modification. The experimenter who made the counts was blinded to all conditions. For DRG cell counts, the images were taken from randomly-chosen areas of DRG slices using 20X objective. The intensity of positively

stained neurons was at least four times higher than the background by setting a threshold according to individual slice and the number of positively stained neurons was counted. The number of total neurons in the same area was counted by DAPI nucleic acid stain. Five to eight slices were chosen for each ganglion. The quantification of immunofluorescent staining in SDH was performed as described before<sup>75</sup>. The intensity of immunohistochemical staining in spinal lamina II was measured after the background fluorescence was subtracted. At least five sections were quantified for each animal. To quantify IENFs, five slices from each animal were randomly chosen. PGP9.5<sup>+</sup> nerve fibers which crossed the collagen-stained dermal/epidermal junction into the epidermis were counted in three fields of view from each slice using a 40x objective (Eclipse E600, Nikon, Japan). The length of the dermal/epidermal border within each field of view was measured and IENF density was determined as the total number of fibers per unit length (IENF/mm)<sup>11</sup>.

### Dissociation of DRG cells and intracellular calcium imaging

Dissociation of rat DRG neurons was performed as previously described<sup>5</sup>. After the completion of chemotherapy (usually 8 – 14 days following treatment), animals were perfused transcardially with cold PBS and L4/L5 DRG of both sides were quickly removed and incubated in DMEM medium containing 2.4 mg/ml collagenase D and 0.4 mg/ml Trypsin at 34°C for 40 min. After being centrifuged and resuspended twice, the cells were then plated on cover slips coated with poly-L-lysine and incubated in DMEM medium at 34°C overnight before further experiments. For intracellular calcium imaging experiments, dissociated DRG cells were loaded with ratiometric Ca<sup>2+</sup> indicator dye Fura-2 AM (2 μM, Molecular Probes) for at least 30 min at 37°C in artificial cerebrospinal fluid (ACSF) containing (mM): 130 NaCl, 24 NaHCO<sub>3</sub>, 3.5 KCl, 1.25 NaH<sub>2</sub>PO<sub>4</sub>, 1.2 MgCl<sub>2</sub>, 1.2 CaCl<sub>2</sub> and 10 Dextrose. The cells were then transferred to a recording chamber placed on the inverted microscope (Nikon Eclipse Ti, Nikon, Japan) and perfused with oxygenated (95% O<sub>2</sub> + 5% CO<sub>2</sub>) ACSF continuously (2 ml/min) at room temperature. The intracellular calcium concentration was expressed as the 340/380 ratio, and the signals were captured and analyzed with Nikon NIS-Elements AR software (Nikon, Japan). All chemicals were directly applied into the bath.

### Statistical analysis

All results are presented as means ± SEM and differences between means were tested for significance using *t*-test, one-way or two-way ANOVA followed by Bonferroni post hoc test with an alpha value of *P* < 0.05.

## RESULTS

### Paclitaxel induces the expression of MCP-1 in both DRG and SDH

The expression of MCP-1 following paclitaxel treatment was examined in detail by immunohistochemistry. MCP-1 immunoreactivity was found markedly increased in DRG in paclitaxel-treated animals (Fig. 1A). The increase in MCP-1 was detected as early as 4 hours after the initiation of the treatment and remained at the peak level through day 7. The level of MCP-1 declined on day 14 but still remained higher in paclitaxel-treated animals than that in vehicle-treated or naïve animals through day 28, the last time point observed (F[2,46] = 197.51, *p* < 0.0001 for treatment factor; F[5,46] = 11, *p* < 0.0001 for time factor; two-way ANOVA, *n* = 4 for naïve; *n* = 3 for both paclitaxel and vehicle at 4h, 24h, 3d and 7d; *n* = 4 for both paclitaxel and vehicle at 14d and 28d) (Fig. 1B). Surprisingly, vehicle-treated animals also showed a transient increase of MCP-1 compared to naïve animals but this difference was significant only at 4 hours and 3 days after treatment (Fig. 1B). Analysis of cell diameter of MCP-1<sup>+</sup> neurons after paclitaxel treatment revealed that the majority of



DRG neurons expressing MCP-1 were small cells ( $< 30\mu\text{m}$ ,  $\sim 83\%$ ,  $n = 457$  out of 545) with a small proportion of medium-sized cells ( $31 \sim 44\mu\text{m}$ ,  $\sim 14\%$ ,  $n = 71$  out of 545) but only very few large cells ( $> 45\mu\text{m}$ ,  $\sim 3\%$ ,  $n = 17$  out of 545) (Fig. 1C). Similar distribution of MCP-1 was observed in the vehicle group but the overall level was much lower (Fig. 1B and C). Double-immunofluorescence further confirmed that the majority of MCP-1<sup>+</sup> neurons were immuno-positive for transient receptor potential cation channel V1 (TRPV1). Both peptidergic (calcitonin gene-related peptide immune-positive, CGRP<sup>+</sup>) and non-peptidergic (isolectin B4 positive, IB4<sup>+</sup>) DRG neurons were found to express MCP-1. A few medium-sized myelinated neurons labeled by neurofilament heavy polypeptide (NF200<sup>+</sup>) were found MCP-1 positive, but large myelinated neurons were rarely found to express MCP-1 (Fig. 1D). These results indicate that the major source of MCP-1 in DRG in paclitaxel CIPN is small unmyelinated neurons, which is in agreement with other models of peripheral neuropathy<sup>7,9,70</sup>.

Paclitaxel also induced a marked increase of MCP-1 in the SDH (Fig. 2A). The protein level of MCP-1 was significantly increased as early as 4 hours and remained at a high level through 14 days after paclitaxel treatment compared to naïve and vehicle groups, but dramatically declined on day 28 ( $F[1,24] = 150.30$ ,  $p < 0.0001$  for treatment factor;  $F[5,24] = 11.99$ ,  $p < 0.0001$  for time factor; two-way ANOVA,  $n = 3$  for naïve, paclitaxel and vehicle groups) (Fig. 2B). Double immunostaining revealed that MCP-1 was induced in spinal astrocytes co-labeled with glial fibrillary acid protein (GFAP<sup>+</sup>), but not in neurons (NeuN<sup>+</sup>) or microglia (OX42<sup>+</sup>) (Fig. 2C). The induction of MCP-1 in spinal astrocytes has also been reported after peripheral nerve injury<sup>23</sup>, and is consistent with the hyperactive phenotype of spinal astrocytes induced by paclitaxel reported previously<sup>75</sup>.

### Paclitaxel induces the expression of CCR2 in DRG but not SDH

MCP-1 preferentially binds to CCR2 to exert its chemotactic effects and induction of CCR2 in DRG neurons has been shown following DRG or peripheral nerve injury<sup>7,9,70</sup>. Hence, the distribution of CCR2 protein in DRG following paclitaxel treatment was next examined. CCR2 was found in a large number of DRG neurons from animals treated with paclitaxel whereas very few cells were found to express CCR2 in vehicle-treated or naïve animals (Fig. 3A). The number of CCR2<sup>+</sup> neurons increased as early as 4 hours, reached a peak level at 7 days and remained elevated through 28 days after paclitaxel treatment ( $F[2,32] = 402.27$ ,  $p < 0.0001$  for treatment factor;  $F[3,32] = 24.14$ ,  $p < 0.0001$  for time factor; two-way ANOVA,  $n = 3, 4$  and  $4$  for naïve, paclitaxel and vehicle at each time point) (Fig. 3B). Different from the expression pattern of MCP-1, the great majority of CCR2<sup>+</sup> cells were myelinated (NF200<sup>+</sup>) DRG neurons and CCR2 was not found in either CGRP<sup>+</sup> or IB4<sup>+</sup> DRG neurons (Fig. 3C).

CCR2-immunoreactivity was not observed in SDH in either naïve, paclitaxel- or vehicle-treated animals (Fig. 3D). Moreover, quantitative real-time polymerase chain reaction (qRT-PCR) revealed an increase in CCR2 messenger RNAs in DRG but not in SDH at both 4 hours and 7 days after the treatment (Fig. 3E), consistent with the change in CCR2 protein in these tissues observed by immunostaining. This observation is in agreement with the previous report that the increase of CCR2 protein and mRNA were found only in DRG but not SDH after peripheral nerve injury<sup>30</sup> (c.f. <sup>23</sup>).

### Expression of MCP-1 and CCR2 in cervical and thoracic DRGs in paclitaxel CIPN

To examine whether the expression of MCP-1 and CCR2 in DRGs maps onto the glove-and-stocking distribution of CIPN symptoms, both proteins were probed in cervical (C7, where skin of partial forepaw is innervated) and mid-thoracic (T5/6) DRGs following paclitaxel treatment. As shown in Fig. 4, the expression of both MCP-1 (Fig. 4A) and CCR2 (Fig. 4B)

were significantly increased in C7 and T5/6 on Day 14 following paclitaxel treatment, compared to vehicle group (n = 3 in each group, *t*-test).

### **MCP-1 induces intracellular calcium increase in DRG neurons following paclitaxel treatment**

CCR2 is a G-protein coupled receptor that when expressed on DRG neurons mediates an increase in intracellular calcium concentration in these cells<sup>7,31,49</sup>. Binding of MCP-1 to CCR2 triggers the release of calcium from intracellular calcium store through the phospholipase-C–phosphatidylinositol 4,5-bisphosphate (PLC-PIP2) pathway<sup>34</sup>. Activation of CCR2 expressed in DRG neurons induced an increase in intracellular calcium concentration after these cells were directly challenged by MCP-1<sup>7,31,49</sup>. Hence, the functional consequence of paclitaxel-induced CCR2 expression on DRG neurons was tested by intracellular calcium imaging. Dissociated DRG neurons were grouped by size and response to capsaicin (0.5 μM). Direct application of MCP-1 (1 μg/ml) induced a prominent increase in intracellular calcium concentration of large and medium-sized DRG neurons from paclitaxel-treated animals. Small DRG neurons which responded to capsaicin did not respond to MCP-1 (Fig. 5A, B). For vehicle-treated animals, the percentage of neurons responding to MCP-1 was 1.9% (1 out of 53), 0% (0 out of 25) and 0.8% (1 out of 125) in large, medium-sized and small neurons, respectively. In paclitaxel-treated animals, the response rate increased to 30.0% (12 out of 40, large), 22.6% (14 out of 62, medium-sized) and 2.6% (3 out of 116, small) (Fig. 5C and Table 1). These results indicate that paclitaxel enhanced the response of large and medium-sized myelinated DRG neurons to MCP-1 after the functional expression of CCR2 was induced in these neurons.

### **Blockade of MCP-1/CCR2 signaling attenuates the mechanical hypersensitivity of paclitaxel CIPN**

The involvement of MCP-1/CCR2 signaling in the generation of the behavioral and anatomical phenotypes of paclitaxel CIPN was further tested by blocking MCP-1/CCR2 signaling. Anti-MCP-1 antibody was first applied by lumbar puncture at the L4-L5 intervertebral space to neutralize any released MCP-1 during chemotherapy. Anti-MCP-1 IgG (500 μg/ml, 10 μl per application) was delivered once daily prior to and during paclitaxel treatment (Fig. 6A). As shown in Figure 6A, animals co-treated with anti-MCP-1 IgG did not develop mechanical hypersensitivity as evidenced by the maintenance of baseline paw withdrawal threshold through the observation interval (16.3 ± 1.5, 18.1 ± 2.6, 15.0 ± 2.8 and 13.5 ± 1.0 gs for baseline, Day 14, 21, and 28, respectively, n = 6). In contrast, animals co-treated in the same fashion with non-specific IgG developed the expected mechanical hypersensitivity induced by paclitaxel as the paw withdrawal threshold dropped from 18.9 ± 2.0 at baseline to 10.4 ± 2.0 at 14 days, 7.6 ± 1.8 at 21 days and 4.7 ± 0.8 gs at 28 days after paclitaxel (n = 7). Vehicle or intrathecal treatment with anti-MCP-1 or non-specific IgGs alone did not cause any changes in paw withdrawal threshold.

To test the role of MCP-1/CCR2 signaling in the maintenance of paclitaxel-induced mechanical hypersensitivity, animals that had fully developed mechanical hypersensitivity were treated intrathecally with CCR2 antisense ODNs to knockdown the expression of CCR2. As shown in Figure 6B, mechanical hypersensitivity was fully developed by day 14 following chemotherapy. Intrathecal delivery of CCR2 antisense but not mismatch ODNs significantly reduced mechanical hypersensitivity as evidenced by the recovery of mechanical threshold. The effect of intrathecal CCR2 antisense ODN quickly diminished after the discontinuation of the treatment. The knockdown of CCR2 was confirmed by immunohistochemical staining that the number of CCR2<sup>+</sup> neurons in DRG was significantly reduced in paclitaxel animals co-treated with antisense but not mismatch ODNs (Fig. 6C).

No significant alteration in motor behavior assessed by rotarod test was observed in any group (data not shown).

### **Blockade of MCP-1/CCR2 signaling prevented the loss of IENFs in paclitaxel CIPN**

CIPN generally appears in a glove-and-stocking distribution with pronounced severity in glabrous skin<sup>37,41</sup>. An anatomical hallmark of CIPN in both patients<sup>12</sup> and animals<sup>11,61</sup> is the loss of IENFs in glabrous skin of the extremities. IENFs are bare nerve endings of A and C fibers after they cross the dermal/epidermal junction and are immuno-positive to protein gene product 9.5 (PGP9.5)<sup>53</sup>. To test if the blockade of MCP-1/CCR2 signaling during the early phase of chemotherapy could prevent the late loss of IENFs, skin biopsy samples from animals co-treated with paclitaxel and anti-MCP-1 antibody were stained with PGP9.5 on day 28 after chemotherapy. Consistent with previous work<sup>11</sup>, a significant decrease in the density of IENFs in skin of hindpaw foot pad was observed in paclitaxel- but not vehicle-treated animals (Fig. 7A). Anti-MCP-1 treatment which has shown to prevent paclitaxel-induced mechanical hypersensitivity also prevented the loss of IENFs (Fig. 7A, B). These results indicate that both behavioral and anatomical phenotypes of paclitaxel CIPN were dependent on the activation of MCP-1/CCR2 signaling in the DRG.

## **DISCUSSION**

Here we show a dynamic role of DRG MCP-1/CCR2 signaling in paclitaxel CIPN. The development of symptoms following paclitaxel chemotherapy has been observed as early as 24 hours in patients<sup>41</sup> and several hours in animals<sup>20</sup>, and may last for weeks to months after repeated treatment<sup>11,20,21,22,41,51</sup>. The early (4 hours, the earliest time point we examined) and persistent (several weeks) induction of MCP-1 and CCR2 following paclitaxel treatment suggests the involvement of MCP-1/CCR2 signaling in both induction and maintenance of paclitaxel CIPN, which was further confirmed by the effects of blocking MCP-1 and CCR2 in preventing and reversing paclitaxel-induced mechanical hypersensitivity. The significant increase in the expression of both MCP-1 and CCR2 found in C7, T5/6 and L4/5 DRGs suggests that the activation of MCP-1/CCR2 signaling might occur in DRGs at all levels following systemic treatment of paclitaxel, and it does not predict the development of the glove-and-stocking distribution of symptoms typically seen in CIPN patients. Additional mechanisms appear to be engaged to generate this anatomical focus.

The finding of newly expressed CCR2 in NF200<sup>+</sup> neurons and MCP-1 in TRPV1<sup>+</sup> neurons suggests that both A- and C-neurons are involved in this response, which is further confirmed by the loss-of-function study showing that both anti-MCP-1 and anti-CCR2 treatment improves paclitaxel-induced pain behavior. Paclitaxel CIPN is characterized by more prominent symptoms of numbness and tingling than shooting/burning pain<sup>21,41</sup>, suggesting a particular impairment of function in large (A<sub>β</sub>) and medium-sized (A<sub>δ</sub>) myelinated fibers and less effect on unmyelinated C fibers<sup>21</sup>. Human psychophysical studies have also shown that tactile allodynia following peripheral nerve injury is mostly mediated by myelinated peripheral afferents<sup>13,42,65</sup>. Increased activities of myelinated A<sub>β</sub>-neurons have been consistently observed in animals with experimental peripheral nerve injury<sup>26,38,40</sup> and suppression of these activities attenuates tactile allodynia<sup>24,38,56</sup>, further suggesting a critical role of these neurons in tactile allodynia. The contribution of A<sub>β</sub>-neurons to central sensitization may be underscored by their de novo expression of substance P, a pronociceptive peptide usually present in C-nociceptors, following peripheral nerve injury<sup>45,46</sup>.

MCP-1 can directly depolarize DRG neurons and even induce action potentials when its cognate receptor CCR2 is expressed on these neurons after injury<sup>62,70</sup>. The paclitaxel-



induced expression of CCR2 in myelinated A and A neurons and consequent activation of intracellular calcium signaling in these neurons by MCP-1 suggests a MCP-1-dependent mechanism in sensitizing myelinated neurons, that is initiated by chemotherapy. The observation that the number of CCR2-expressing DRG neurons is significantly increased following chemotherapy while CCR2-expressing neurons are rarely found in vehicle-treated or naïve animals is consistent with other studies that the level of CCR2 in DRG is very low in intact animals while markedly increased following injury or inflammation<sup>7,9,30,70</sup>. Although it has been reported that dissociated DRG neurons, especially small and medium-sized cells, from naïve animals express CCR2 and respond to MCP-1 by increasing tetrodotoxin-resistant sodium current<sup>6</sup>, we only observed a very small number of neurons dissociated from vehicle-treated animals which responded to MCP-1 with intracellular calcium increases. This difference in effects may be a result of different methods used to dissociate the target DRG neurons, such as variant digesting times and whether bovine serum is in the medium.

Interestingly, MCP-1, the chemokine most active at CCR2, was found to be induced in small unmyelinated DRG neurons following paclitaxel treatment, suggesting a contribution of C-neurons to paclitaxel CIPN. The MCP-1-expressing DRG neurons included both IB4 positive and CGRP positive cells. Many signaling molecules and neuropeptides such as Substance P<sup>29</sup>, ATP<sup>77</sup>, CGRP<sup>50</sup> and MCP-1<sup>31</sup> can be released from DRG somata upon depolarization through both Ca<sup>2+</sup>-dependent and -independent mechanisms<sup>39,74</sup>. The release of MCP-1 from the somata of C-neurons in CIPN could be triggered by spontaneous activity in these fibers that arises at either the soma or peripheral endings<sup>71</sup>. Unlike other types of neuropathy where MCP-1 and CCR2 are primarily expressed in the same nociceptive neurons<sup>9,30,70</sup>, paclitaxel induced MCP-1 was observed in small, presumably unmyelinated neurons whereas CCR2 was observed in large myelinated neurons. This suggests the possibility that a paracrine MCP-1/CCR2 signaling process occurs in CIPN instead of an autocrine mechanism that may be more prevalent in traumatic neuropathic conditions<sup>3,19,48</sup>.

The increased expression of MCP-1 in spinal astrocytes reflects the persistent hyper-reactive status of astrocytes following paclitaxel treatment, which is confirmed by the increased expression of GFAP, an astrocyte marker, following chemotherapy<sup>75</sup>. Peripheral nerve injury has been shown to induce MCP-1 in astrocytes of spinal and medullary dorsal horn<sup>23,78</sup>. Spinal release of MCP-1 following chronic constriction injury to the sciatic nerve induces production of pro-inflammatory cytokines such as interleukin-1 and interleukin-6 and activation of extracellular signal-regulated kinase 1/2 (ERK) in the spinal dorsal horn<sup>66</sup>. Although a few CCR2-expressing neurons have been found concomitantly following nerve injury in those studies<sup>23,78</sup>, we did not detect CCR2 protein or increase of CCR2 mRNA in lumbar spinal cord following paclitaxel treatment, indicating a different pattern of CCR2 expression between nerve injury and chemotherapy. Lack of CCR2 in SDH strongly suggests that therapeutic effects of intrathecal anti MCP-1 or CCR2 treatment will target the DRG rather than the SDH.

Another striking finding is that pre-emptive treatment with anti-MCP-1 antibody prevented chemotherapy-induced loss of IENFs. IENFs originate from C- and A -neurons and loss of IENFs has been consistently observed in patients who develop chronic peripheral neuropathy following chemotherapy<sup>12,55</sup> as well as diabetic neuropathy<sup>32</sup>, HIV-associated neuropathy<sup>52</sup>, postherpetic neuropathy<sup>57</sup> and peripheral neuropathy following injury<sup>27,60</sup>. The prevention of IENF loss by blocking MCP-1/CCR2 signaling strongly suggests an unidentified feedback signal from A-neurons affecting C- and A -neurons.

In summary, we have shown that a novel signaling pathway mediated by MCP-1/CCR2 between myelinated- and unmyelinated-neurons appears to be induced by paclitaxel within the DRG and blocking MCP-1/CCR2 signaling prevents the development of paclitaxel CIPN phenotypes including mechanical hypersensitivity and loss of IENFs. Interactions between DRG neurons mediated by MCP-1/CCR2, possibly through a paracrine route, may be a key part of paclitaxel-induced ganglionopathy which ultimately leads to CIPN. There are certainly questions that need further study, such as the specific signals/molecules involved in the loss of IENFs, the basis for the striking glove-and-stocking pattern of CIPN, and the signals that are upstream and downstream of MCP-1/CCR2. Nevertheless, our results suggest that a novel strategy of targeting MCP-1 and/or CCR2 could be a promising therapy for paclitaxel CIPN which could be evaluated in future clinical studies.

## Acknowledgments

This work was supported by grants from National Institutes of Health (NS 046606), National Cancer Institute (CA12487) and by the Astra-Zeneca Corporation.

## References

1. Abbadie C, Lindia JA, Cumiskey AM, Peterson LB, Mudgett JS, Bayne EK, DeMartino JA, MacIntyre DE, Forrest MJ. Impaired neuropathic pain responses in mice lacking the chemokine receptor CCR2. *Proc Natl Acad Sci USA*. 2003; 100:7947–7952. [PubMed: 12808141]
2. Alessandri-Haber N, Yeh JJ, Boyd AE, Parada CA, Chen X, Reichling DB, Levine JD. Hypotonicity induces TRPV4-mediated nociception in rat. *Neuron*. 2003; 39:497–511. [PubMed: 12895423]
3. Amir R, Devor M. Chemically mediated cross-excitation in rat dorsal root ganglia. *J Neurosci*. 1996; 16:4733–4741. [PubMed: 8764660]
4. Archer DR, Dahlin LB, McLean WG. Changes in slow axonal transport of tubulin induced by local application of colchicine to rabbit vagus nerve. *Acta Physiol Scand*. 1994; 150:57–65. [PubMed: 7510922]
5. Bedi SS, Yang Q, Crook RJ, Du J, Wu Z, Fishman HM, Grill RJ, Carlton SM, Walters ET. Chronic spontaneous activity generated in the somata of primary nociceptors is associated with pain-related behavior after spinal cord injury. *J Neurosci*. 2010; 30:14870–14882. [PubMed: 21048146]
6. Belkouch M, Dansereau MA, Reaux-Le GA, Van SJ, Beaudet N, Chraïbi A, Melik-Parsadaniantz S, Sarret P. The chemokine CCL2 increases Nav1.8 sodium channel activity in primary sensory neurons through a Gbetagamma-dependent mechanism. *J Neurosci*. 2011; 31:18381–18390. [PubMed: 22171040]
7. Bhangoo S, Ren D, Miller RJ, Henry KJ, Lineswala J, Hamdouchi C, Li B, Monahan PE, Chan DM, Ripsch MS, White FA. Delayed functional expression of neuronal chemokine receptors following focal nerve demyelination in the rat: a mechanism for the development of chronic sensitization of peripheral nociceptors. *Mol Pain*. 2007; 3:38. [PubMed: 18076762]
8. Bhangoo SK, Ren D, Miller RJ, Chan DM, Ripsch MS, Weiss C, McGinnis C, White FA. CXCR4 chemokine receptor signaling mediates pain hypersensitivity in association with antiretroviral toxic neuropathy. *Brain Behav Immun*. 2007; 21:581–591. [PubMed: 17292584]
9. Bhangoo SK, Ripsch MS, Buchanan DJ, Miller RJ, White FA. Increased chemokine signaling in a model of HIV1-associated peripheral neuropathy. *Mol Pain*. 2009; 5:48. [PubMed: 19674450]
10. Bogen O, Dina OA, Gear RW, Levine JD. Dependence of monocyte chemoattractant protein 1 induced hyperalgesia on the isolectin B4-binding protein versican. *Neuroscience*. 2009; 159:780–786. [PubMed: 19167466]
11. Boyette-Davis J, Xin W, Zhang H, Dougherty PM. Intraepidermal nerve fiber loss corresponds to the development of Taxol-induced hyperalgesia and can be prevented by treatment with minocycline. *Pain*. 2011; 152:308–313. [PubMed: 21145656]

12. Boyette-Davis JA, Cata JP, Zhang H, Driver LC, Wendelschafer-Crabb G, Kennedy WR, Dougherty PM. Follow-up psychophysical studies in bortezomib-related chemoneuropathy patients. *J Pain*. 2011; 12:1017–1024. [PubMed: 21703938]
13. Campbell JN, Raja SN, Meyer RA, Mackinnon SE. Myelinated afferents signal the hyperalgesia associated with nerve injury. *Pain*. 1988; 32:89–94. [PubMed: 3340426]
14. Cata JP, Weng HR, Dougherty PM. The effects of thalidomide and minocycline on taxol-induced hyperalgesia in rats. *Brain Res*. 2008; 1229:100–110. [PubMed: 18652810]
15. Cavaletti G, Marmiroli P. Chemotherapy-induced peripheral neurotoxicity. *Nat Rev Neurol*. 2010; 6:657–666. [PubMed: 21060341]
16. Chaplan SR, Bach FW, Pogrel JW, Chung JM, Yaksh TL. Quantitative assessment of tactile allodynia in the rat paw. *J Neurosci Meth*. 1994; 53:55–63.
17. Dahlstrom A: Effect of colchicine on transport of amine storage granules in sympathetic nerve of rat. *Eur J Pharmacol*. 1968; 5:111–113. [PubMed: 5718512]
18. De la Calle JL, Paino CL. A procedure for direct lumbar puncture in rats. *Brain Res Bull*. 2002; 59:245–250. [PubMed: 12431755]
19. Devor M, Wall PD. Cross-excitation in dorsal root ganglia of nerve-injured and intact rats. *J Neurophysiol*. 1990; 64:1733–1745. [PubMed: 2074461]
20. Dina OA, Chen X, Reichling D, Levine JD. Role of protein kinase C[epsilon] and protein kinase A in a model of paclitaxel-induced painful peripheral neuropathy in the rat. *Neuroscience*. 2001; 108:507–515. [PubMed: 11738263]
21. Dougherty PM, Cata JP, Cordella JV, Burton A, Weng H-R. Taxol-induced sensory disturbance is characterized by preferential impairment of myelinated fiber function in cancer patients. *Pain*. 2004; 109:132–142. [PubMed: 15082135]
22. Flatters SJ, Bennett GJ. Studies of peripheral sensory nerves in paclitaxel-induced painful peripheral neuropathy evidence for mitochondrial dysfunction. *Pain*. 2006; 122:245–257. [PubMed: 16530964]
23. Gao YJ, Zhang L, Samad OA, Suter MR, Yasuhiko K, Xu ZZ, Park JY, Lind AL, Ma Q, Ji RR. JNK-Induced MCP-1 Production in Spinal Cord Astrocytes Contributes to Central Sensitization and Neuropathic Pain. *J Neurosci*. 2009; 29:4096–4108. [PubMed: 19339605]
24. Gracely RH, Lynch SA, Bennett GJ. Painful neuropathy altered central processing maintained dynamically by peripheral input. *Pain*. 1992; 51:175–194. [PubMed: 1484715]
25. Guo W, Wang H, Zou S, Dubner R, Ren K. Chemokine signaling involving chemokine (CC motif) ligand 2 plays a role in descending pain facilitation. *Neurosci Bull*. 2012; 28:193–207. [PubMed: 22466130]
26. Han HC, Lee DH, Chung JM. Characteristics of ectopic discharges in a rat neuropathic pain model. *Pain*. 2000; 84:253–261. [PubMed: 10666530]
27. Holland NR, Stocks A, Hauer P, Cornblath DR, Griffin JW, McArthur JC. Intraepidermal nerve fiber density in patients with painful sensory neuropathy. *Neurology*. 1997; 48:708–711. [PubMed: 9065552]
28. Horie H, Takenaka T, Ito S, Kim SU. Taxol counteracts colchicine blockade of axonal transport in neurites of cultured dorsal root ganglion cells. *Brain Res*. 1987; 420:144–146. [PubMed: 2445429]
29. Huang LY, Neher E. Ca(2+)-dependent exocytosis in the somata of dorsal root ganglion neurons. *Neuron*. 1996; 17:135–145. [PubMed: 8755485]
30. Jung H, Bhargoo S, Banisadr G, Freitag G, Ren D, White FA, Miller RJ. Visualization of chemokine receptor activation in transgenic mice reveals peripheral activation of CCR2 receptors in states of neuropathic pain. *J Neurosci*. 2009; 29:8051–8062. [PubMed: 19553445]
31. Jung H, Toth PT, White FA, Miller RJ. Monocyte chemoattractant protein-1 functions as a neuromodulator in dorsal root ganglia neurons. *J Neurochem*. 2008; 104:254–263. [PubMed: 17944871]
32. Kennedy WR, Wendelschafer-Crabb G, Johnson T. Quantitation of epidermal nerves in diabetic neuropathy. *Neurology*. 1996; 47:1042–1048. [PubMed: 8857742]
33. Kingery WS, Guo TZ, Poree LR, Maze M. Colchicine treatment of the sciatic nerve reduces neurogenic extravasation, but does not affect nociceptive thresholds or collateral sprouting in neuropathic rats. *Pain*. 1998; 74:11–20. [PubMed: 9514555]

34. Kuang Y, Wu Y, Jiang H, Wu D. Selective G protein coupling by C-C chemokine receptors. *J Biol Chem.* 1996; 271:3975–3978. [PubMed: 8626727]
35. Lacroix-Fralish ML, Austin JS, Zheng FY, Levitin DJ, Mogil JS. Patterns of pain meta-analysis of microarray studies of pain. *Pain.* 2011; 152:1888–1898. [PubMed: 21561713]
36. Lai J, Gold MS, Kim CS, Bian D, Ossipov MH, Hunter JC, Porreca F. Inhibition of neuropathic pain by decreased expression of the tetrodotoxin-resistant sodium channel, NaV1.8. *Pain.* 2002; 95:143–152. [PubMed: 11790477]
37. Lee JJ, Swain SM. Peripheral neuropathy induced by microtubule-stabilizing agents. *J Clin Oncol.* 2006; 24:1633–1642. [PubMed: 16575015]
38. Liu C-N, Wall PD, Ben-Dor E, Michaelis M, Amir R, Devor M. Tactile allodynia in the absence of C-fiber activation: altered firing properties of DRG neurons following spinal nerve injury. *Pain.* 2000; 85:503–521. [PubMed: 10781925]
39. Liu T, Shang SJ, Liu B, Wang CH, Wang YS, Xiong W, Zheng LH, Zhang CX, Zhou Z. Two distinct vesicle pools for depolarization-induced exocytosis in somata of dorsal root ganglion neurons. *J Physiol.* 2011; 589:3507–3515. [PubMed: 21646411]
40. Liu X, Eschenfelder S, Blenk KH, Janig W, Habler H. Spontaneous activity of axotomized afferent neurons after L5 spinal nerve injury in rats. *Pain.* 2000; 84:309–318. [PubMed: 10666536]
41. Loprinzi CL, Reeves BN, Dakhil SR, Sloan JA, Wolf SL, Burger KN, Kamal A, Le-Lindqwister NA, Soori GS, Jaslowski AJ, Novotny PJ, Lachance DH. Natural history of paclitaxel-associated acute pain syndrome: prospective cohort study NCCTG N08C1. *J Clin Oncol.* 2011; 29:1472–1478. [PubMed: 21383290]
42. Magerl W, Fuchs PN, Meyer RA, Treede RD. Roles of capsaicin-insensitive nociceptors in cutaneous pain and secondary hyperalgesia. *Brain.* 2001; 124:1754–1764. [PubMed: 11522578]
43. Matsuka Y, Neubert JK, Maidment NT, Spigelman I. Concurrent release of ATP and substance P within guinea pig trigeminal ganglia in vivo. *Brain Res.* 2001; 915:248–255. [PubMed: 11595216]
44. Myers RR, Campana WM, Shubayev VI. The role of neuroinflammation in neuropathic pain: mechanisms and therapeutic targets. *Drug Discov Today.* 2006; 11:8–20. [PubMed: 16478686]
45. Neumann S, Doubell TP, Leslie T, Woolf CJ. Inflammatory pain hypersensitivity mediated by phenotypic switch in myelinated primary sensory neurons. *Nature.* 1996; 384:360–364. [PubMed: 8934522]
46. Noguchi K, Kawai Y, Fukuoka T, Senba E, Miki K. Substance p induced by peripheral nerve injury in primary afferent sensory neurons and its effects on dorsal column nucleus neurons. *J Neurosci.* 1995; 15:7633–7643. [PubMed: 7472514]
47. Ogawa T, Mimura Y, Isowa K, Kato H, Mitsuishi M, Toyoshi T, Kuwayama N, Morimoto H, Murakoshi T, Nakayama T. An antimicrotubule agent, TZT-1027, does not induce neuropathologic alterations which are detected after administration of vincristine or paclitaxel in animal models. *Toxicol Lett.* 2001; 121:97–106. [PubMed: 11325560]
48. Oh EJ, Weinreich D. Chemical communication between vagal afferent somata in nodose Ganglia of the rat and the Guinea pig in vitro. *J Neurophysiol.* 2002; 87:2801–2807. [PubMed: 12037182]
49. Oh SB, Tran PB, Gillard SE, Hurley RW, Hammond DL, Miller RJ. Chemokines and glycoprotein 120 produce pain hypersensitivity by directly exciting primary nociceptive neurons. *J Neurosci.* 2001; 21:5027–5035. [PubMed: 11438578]
50. Ouyang K, Zheng H, Qin X, Zhang C, Yang D, Wang X, Wu C, Zhou Z, Cheng H. Ca<sup>2+</sup> sparks and secretion in dorsal root ganglion neurons. *Proc Natl Acad Sci U S A.* 2005; 102:12259–12264. [PubMed: 16103366]
51. Polomano RC, Mannes AJ, Clark US, Bennett GJ. A painful peripheral neuropathy in the rat produced by the chemotherapeutic drug, paclitaxel. *Pain.* 2001; 94:293–304. [PubMed: 11731066]
52. Polydefkis M, Yiannoutsos CT, Cohen BA, Hollander H, Schifitto G, Clifford DB, Simpson DM, Katzenstein D, Shriver S, Hauer P, Brown A, Haidich AB, Moo L, McArthur JC. Reduced intraepidermal nerve fiber density in HIV-associated sensory neuropathy. *Neurology.* 2002; 58:115–119. [PubMed: 11781415]
53. Rice, FL.; Albercht, PJ. Cutaneous Mechanisms of Tactile Perception: Morphological and Chemical Organization of the Innervation to the Skin. In: Kaas, J.; Gardner, E.; Basbaum, A.; Kaneko, A.; Shepherd, G.; Westheimer, G.; Albright, T.; Masland, R.; Dallos, P.; Oertel, D.;

- Firestein, S.; Beauchamp, G.; Bushnell, C., editors. *The Senses: A Comprehensive Reference*. Oxford: 2008. p. 1-31.
54. Richards N, Batty T, Dilley A. CCL2 has similar excitatory effects to TNF-alpha in a subgroup of inflamed C-fiber axons. *J Neurophysiol*. 2011; 106:2838–2848. [PubMed: 21865436]
  55. Richardson PG, Xie W, Mitsiades C, Chanan-Khan AA, Lonial S, Hassoun H, Avigan DE, Oaklander AL, Kuter DJ, Wen PY, Kesari S, Briemberg HR, Schlossman RL, Munshi NC, Heffner LT, Doss D, Esseltine DL, Weller E, Anderson KC, Amato AA. Single-agent bortezomib in previously untreated multiple myeloma: efficacy, characterization of peripheral neuropathy, and molecular correlations with response and neuropathy. *J Clin Oncol*. 2009; 27:3518–3525. [PubMed: 19528374]
  56. Rowbotham MC, Fields HL. The relationship of pain, allodynia and thermal sensation in post-herpetic neuralgia. *Brain*. 1996; 119:347–354. [PubMed: 8800931]
  57. Rowbotham MC, Yosipovitch G, Connolly MK, Finlay D, Forde G, Fields HL. Cutaneous innervation density in the allodynic form of postherpetic neuralgia. *Neurobiology of Disease*. 1996; 3:204–214.
  58. Sandler SG, Tobin W, Henderson ES. Vincristine-induced neuropathy. A clinical study of fifty leukemic patients. *Neurology*. 1969; 19:367–374. [PubMed: 5813374]
  59. Schmittgen TD, Livak KJ. Analyzing real-time PCR data by the comparative C(T) method. *Nat Protoc*. 2008; 3:1101–1108. [PubMed: 18546601]
  60. Schuning J, Scherens A, Haussleiter IS, Schwenkreis P, Krumova EK, Richter H, Maier C. Sensory changes and loss of intraepidermal nerve fibers in painful unilateral nerve injury. *Clin J Pain*. 2009; 25:683–690. [PubMed: 19920717]
  61. Siau C, Xiao W, Bennett GJ. Paclitaxel-and vincristine-evoked painful peripheral neuropathies: Loss of epidermal innervation and activation of Langerhans cells. *Exp Neurol*. 2006; 201:507–514. [PubMed: 16797537]
  62. Sun JH, Yang B, Donnelly DF, Ma C, LaMotte RH. MCP-1 enhances excitability of nociceptive neurons in chronically compressed dorsal root ganglia. *J Neurophysiol*. 2006; 96:2189–2199. [PubMed: 16775210]
  63. Tanaka T, Minami M, Nakagawa T, Satoh M. Enhanced production of monocyte chemoattractant protein-1 in the dorsal root ganglia in a rat model of neuropathic pain: possible involvement in the development of neuropathic pain. *Neuroscience Research*. 2004; 48:463–469. [PubMed: 15041200]
  64. Thacker MA, Clark AK, Bishop T, Grist J, Yip PK, Moon LD, Thompson SW, Marchand F, McMahon SB. CCL2 is a key mediator of microglia activation in neuropathic pain states. *Eur J Pain*. 2009; 13:263–272. [PubMed: 18554968]
  65. Torebjork HE, Lundberg LER, LaMotte RH. Central changes in processing of mechanoreceptive input in capsaicin-induced secondary hyperalgesia in humans. *J Physiol*. 1992; 448:765–780. [PubMed: 1593489]
  66. Van SJ, Reaux-Le GA, Pommier B, Mauborgne A, Dansereau MA, Kitabgi P, Sarret P, Pohl M, Melik PS. CCL2 released from neuronal synaptic vesicles in the spinal cord is a major mediator of local inflammation and pain after peripheral nerve injury. *J Neurosci*. 2011; 31:5865–5875. [PubMed: 21490228]
  67. Wang XM, Lehky TJ, Brell JM, Dorsey SG. Discovering cytokines as targets for chemotherapy-induced painful peripheral neuropathy. *Cytokine*. 2012; 59:3–9. [PubMed: 22537849]
  68. Weiden PL, Wright SE. Vincristine Neurotoxicity. *New Eng J Med*. 1972; 286:1369–1370. [PubMed: 5027400]
  69. White FA, Bhargoo SK, Miller RJ. Chemokines integrators of pain and inflammation. *Nat Rev Drug Discov*. 2005; 4:834–844. [PubMed: 16224455]
  70. White FA, Sun J, Waters SM, Ma C, Ren D, Ripsch M, Steflink J, Cortright DN, LaMotte RH, Miller RJ. Excitatory monocyte chemoattractant protein-1 signaling is up-regulated in sensory neurons after chronic compression of the dorsal root ganglion. *Proc Natl Acad Sci U S A*. 2005; 102:14092–14097. [PubMed: 16174730]



71. Xiao WH, Bennett GJ. Chemotherapy-evoked neuropathic pain: Abnormal spontaneous discharge in A-fiber and C-fiber primary afferent neurons and its suppression by acetyl-Lcarnitine. *Pain*. 2008; 135:262–270. [PubMed: 17659836]
72. Xu JJ, Walla BC, Diaz MF, Fuller GN, Gutstein HB. Intermittent lumbar puncture in rats: a novel method for the experimental study of opioid tolerance. *Anesth Analg*. 2006; 103:714–720. [PubMed: 16931686]
73. Younger DS, Mayer SA, Weimer LH, Alderson LM, Sepowitz AH, Lovelace RE. Colchicine-induced myopathy and neuropathy. *Neurology*. 1991; 41:943–944. [PubMed: 2046950]
74. Zhang C, Zhou Z. Ca<sup>2+</sup>-independent but voltage-dependent secretion in mammalian dorsal root ganglion neurons. *Nat Neurosci*. 2002; 5:425–430. [PubMed: 11953753]
75. Zhang H, Yoon S-Y, Zhang H, Dougherty PM. Evidence that spinal astrocytes but not microglia contribute to the pathogenesis of paclitaxel-induced painful neuropathy. *J Pain*. 2012; 13:293–303. [PubMed: 22285612]
76. Zhang J, De Koninck Y. Spatial and temporal relationship between monocyte chemoattractant protein-1 expression and spinal glial activation following peripheral nerve injury. *J Neurochem*. 2006; 97:772–783. [PubMed: 16524371]
77. Zhang X, Chen Y, Wang C, Huang LY. Neuronal somatic ATP release triggers neuron-satellite glial cell communication in dorsal root ganglia. *Proc Natl Acad Sci U S A*. 2007; 104:9864–9869. [PubMed: 17525149]
78. Zhang ZJ, Dong YL, Lu Y, Cao S, Zhao ZQ, Gao YJ. Chemokine CCL2 and its receptor CCR2 in the medullary dorsal horn are involved in trigeminal neuropathic pain. *J Neuroinflammation*. 2012; 9:136. [PubMed: 22721162]

**PERSPECTIVE**

CIPN is a severe side effect accompanying paclitaxel chemotherapy and lacks effective treatments. The current study suggests that blocking MCP-1/CCR2 signaling could be a new therapeutic strategy to prevent or reverse paclitaxel CIPN. This preclinical evidence encourages future clinical evaluation of this strategy.

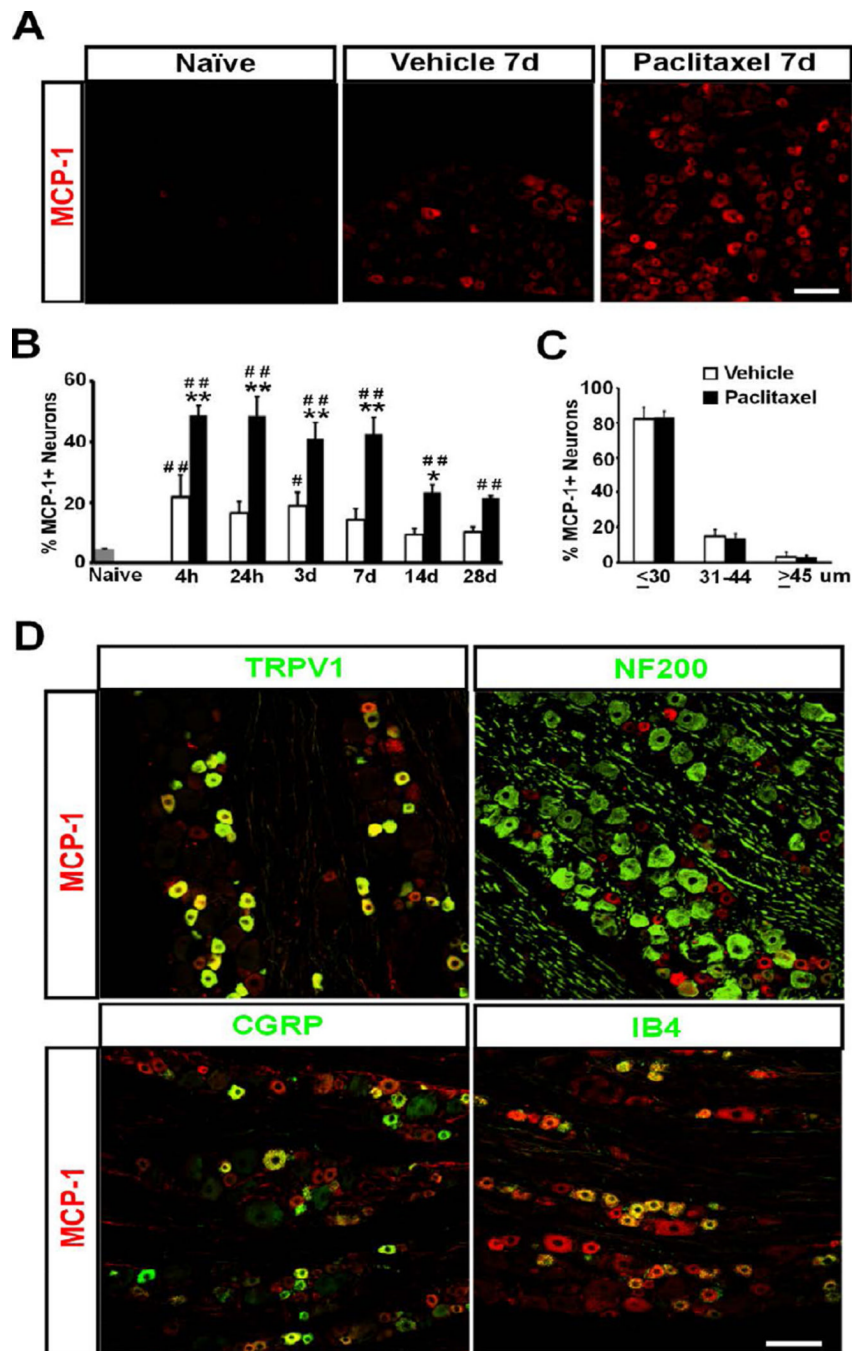


**Figure 1.** The induction of MCP-1 in DRG by Paclitaxel. **A.** Immunostaining shows marked upregulation of MCP-1 in DRG neurons from paclitaxel-treated animals compared to vehicle-treated or naïve animals. **B.** The increase of MCP-1 is observed as early as 4 hours and persists through 28 days after treatment. **C.** The distribution of MCP-1<sup>+</sup> neurons in DRG at 4 hours after paclitaxel or vehicle treatment shows the majority of MCP-1<sup>+</sup> neurons is small cells. **D.** MCP-1<sup>+</sup> (red) neurons are co-labeled (yellow) with TRPV1 (green), CGRP (green) and IB4 (green), but minimally with NF200 (green). \*  $p < 0.05$ , \*\*  $p < 0.01$  versus vehicle; #  $p < 0.05$ , ##  $p < 0.01$  versus naïve. Scale bar: 100  $\mu$ m.

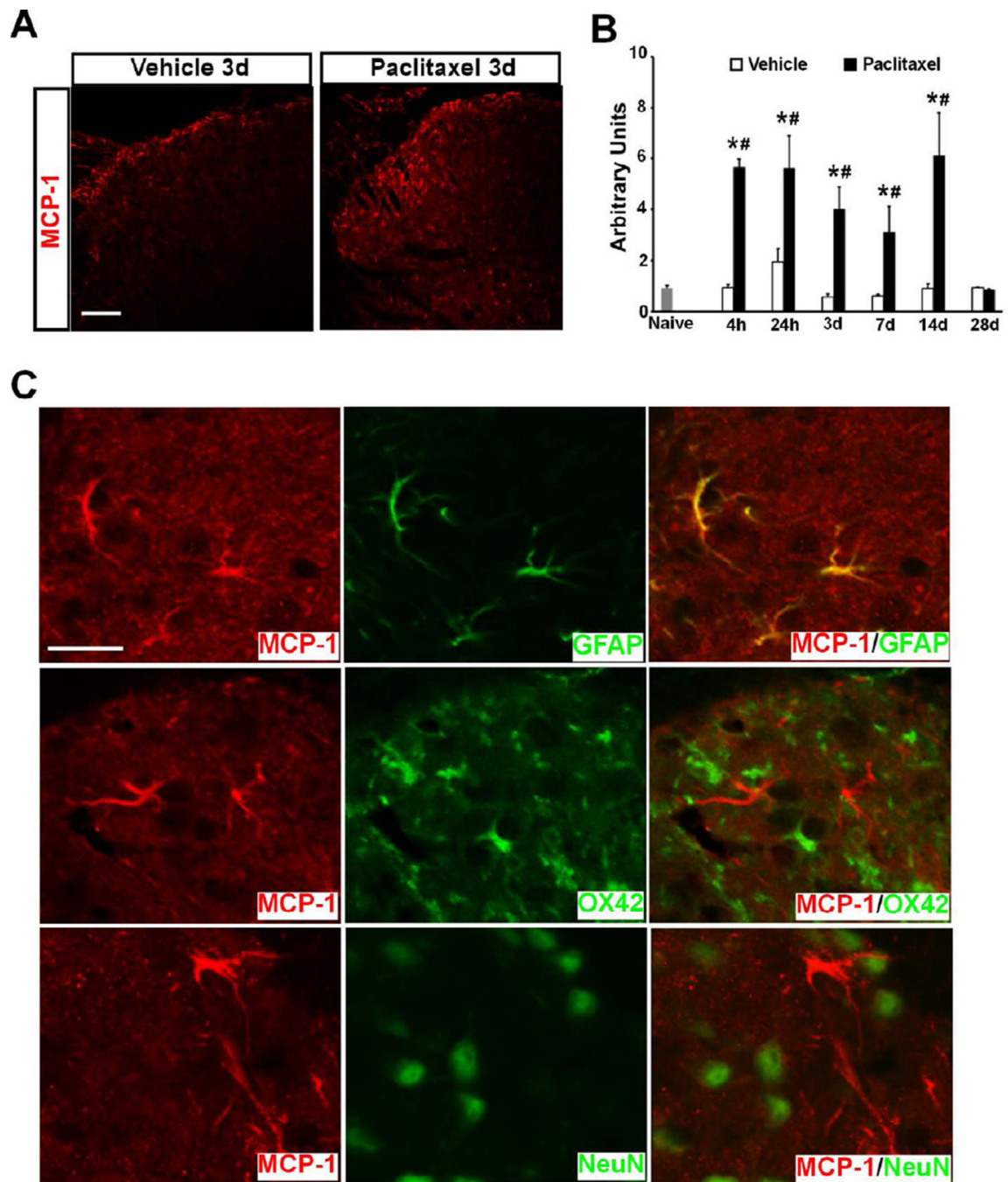


**Figure 2.**

The induction of MCP-1 in SDH by Paclitaxel. **A.** Immunostaining shows marked upregulation of MCP-1 in SDH following paclitaxel treatment. **B.** The increase of MCP-1 is observed as early as 4 hours and persists through 14 days after treatment. **C.** Double immunostaining shows MCP-1 (red) is induced in spinal astrocytes (green) but not neurons (green) or microglia (green). \*  $p < 0.01$  versus vehicle; #  $p < 0.01$  versus naive. Scale bar: 100  $\mu\text{m}$  (A) and 20  $\mu\text{m}$  (C).



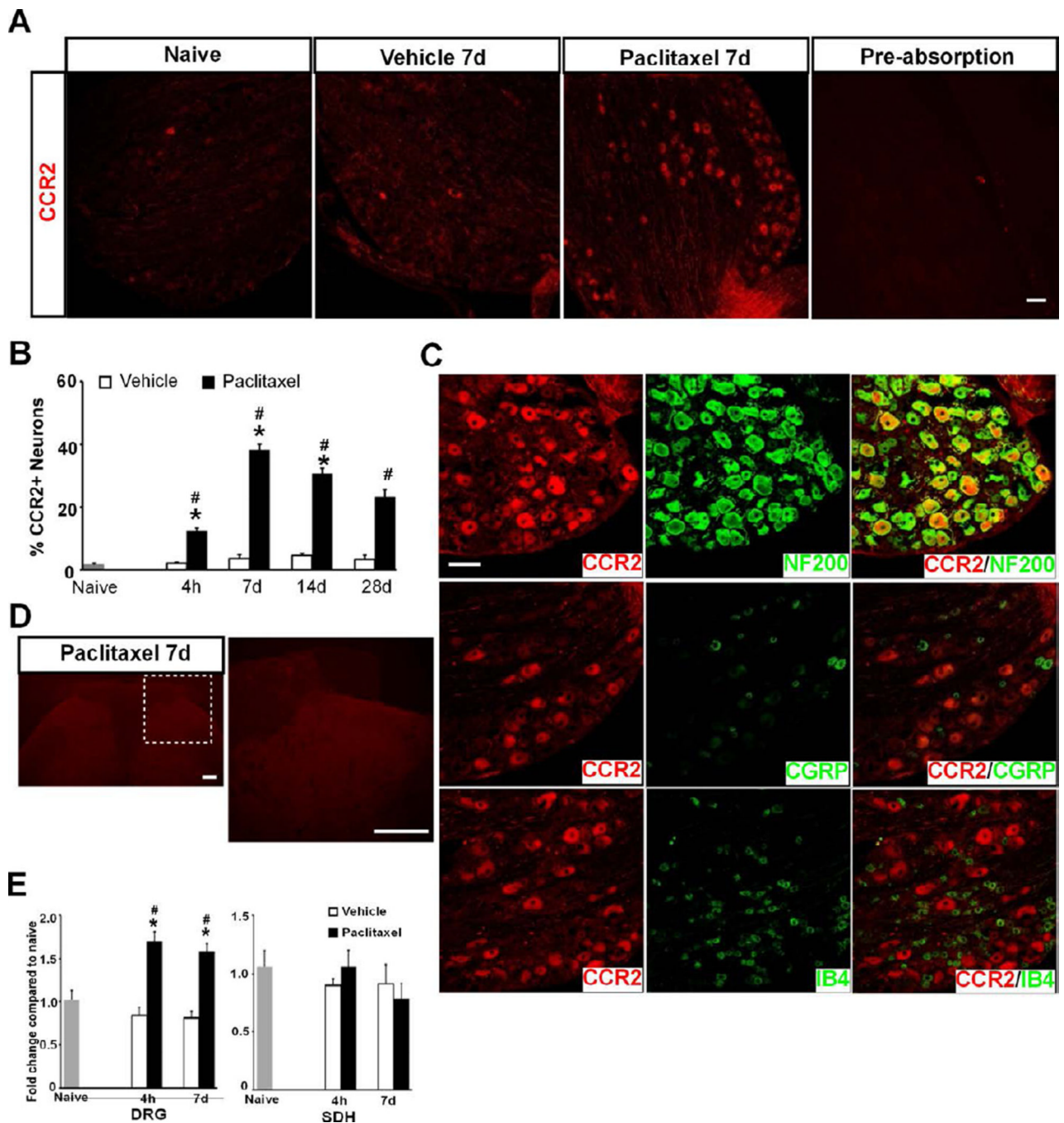


**Figure 3.**

Paclitaxel induces expression of CCR2 in DRG but not SDH. **A.** Immunostaining shows marked upregulation of CCR2 in DRG neurons from paclitaxel- but not vehicle-treated or naïve animals. Pre-absorption of CCR2 blocked the immunohistochemical staining of DRG. **B.** The increase of CCR2 is observed as early as 4 hours and persists through 28 days after treatment. **C.** CCR2<sup>+</sup> (red) neurons are co-labeled (yellow) with NF200 (green) but not with CGRP (green) or IB4 (green). **D.** No signal of CCR2 is detected by immunostaining in SDH after either paclitaxel or vehicle treatment. **E.** Paclitaxel induces an increase in mRNA of CCR2 in DRG ( $F[2,34] = 40.05$ ,  $p < 0.0001$ , two-way ANOVA,  $n = 4, 8$  and  $8$  for naïve,



paclitaxel or vehicle at both time points) but not SDH at 4 hours and 7 days following treatment. \*  $p < 0.0001$  versus vehicle; #  $p < 0.001$  versus naïve. Scale bar: 100  $\mu\text{m}$  (**A** and **C**) and 200  $\mu\text{m}$  (**D**).

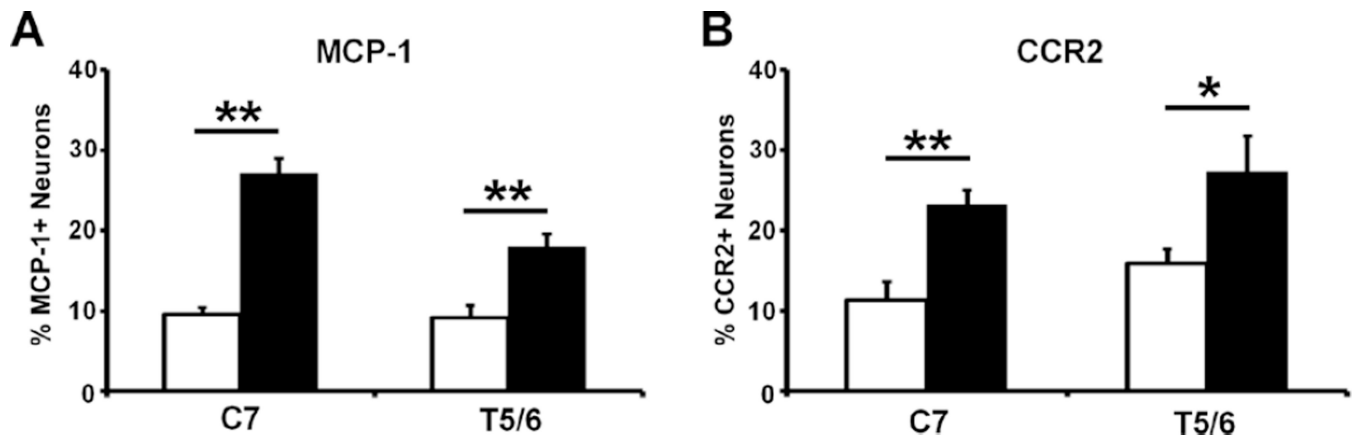


**Figure 4.** Paclitaxel induces the prominent expression of MCP-1 (A) and CCR2 (B) in both C7 and T5/6 DRGs. Tissues were examined on day 14 after chemotherapy. \*  $p < 0.05$ , \*\*  $p < 0.01$ , paclitaxel versus vehicle,  $t$ -test,  $n = 3$  each group.

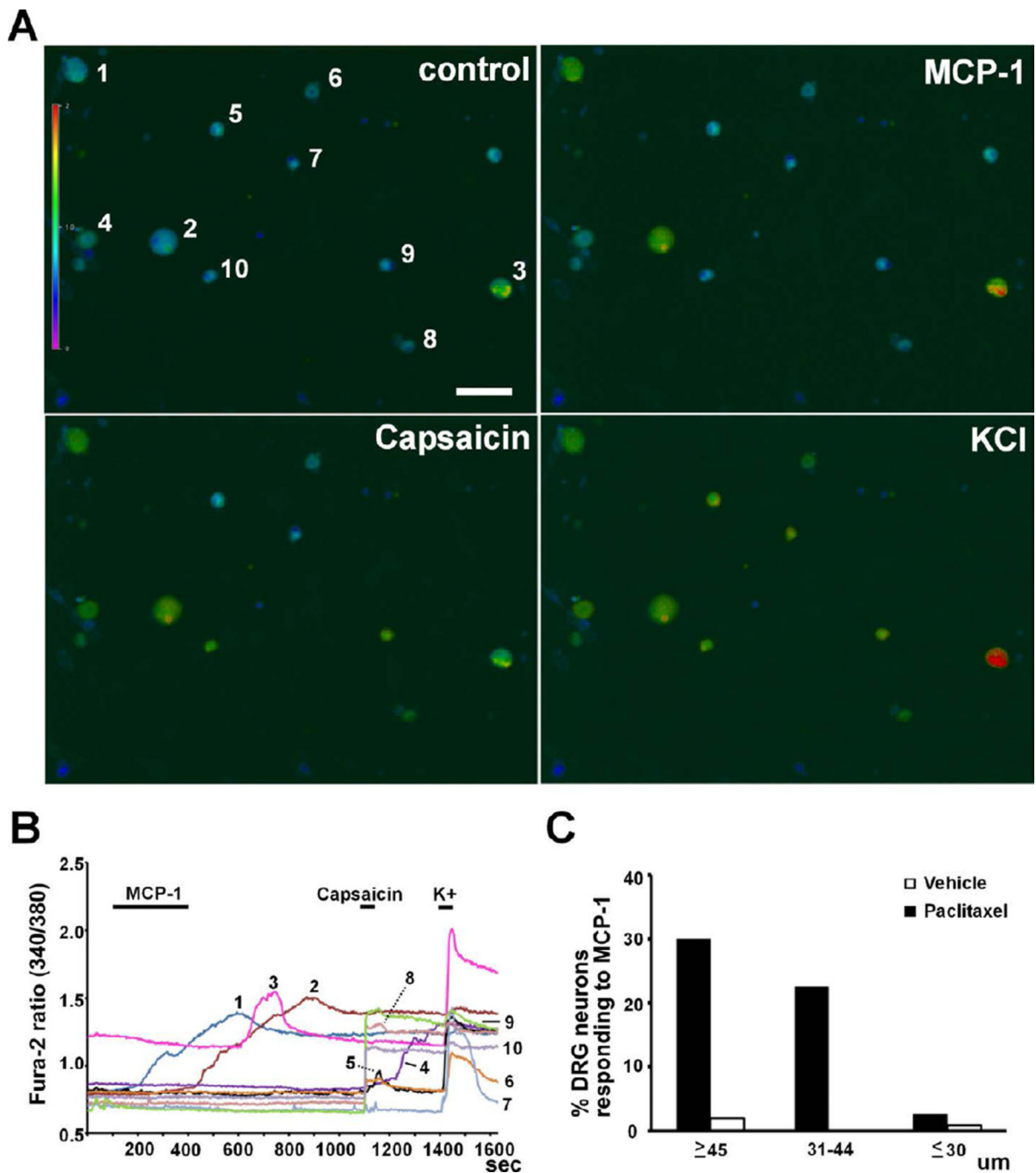


**Figure 5.**

Intracellular calcium response of DRG neurons to MCP-1. **A, B.** MCP-1 (1  $\mu\text{g/ml}$ ) induced increases in intracellular calcium concentration in large (#1 and 2) and medium-sized (#3) neurons which did not respond to capsaicin (0.5  $\mu\text{M}$ ) but did respond to a high concentration of  $\text{K}^+$  (50 mM). Small neurons did not respond to MCP-1 but responded to capsaicin and  $\text{K}^+$  (#4, 5, 6, 8, 9 and 10). One small neuron did not respond to MCP-1 or capsaicin but responded to  $\text{K}^+$  (#7). **C.** Size distribution of DRG neurons responding to MCP-1 from paclitaxel- and vehicle-treated animals. Scale bar: 100  $\mu\text{m}$ .

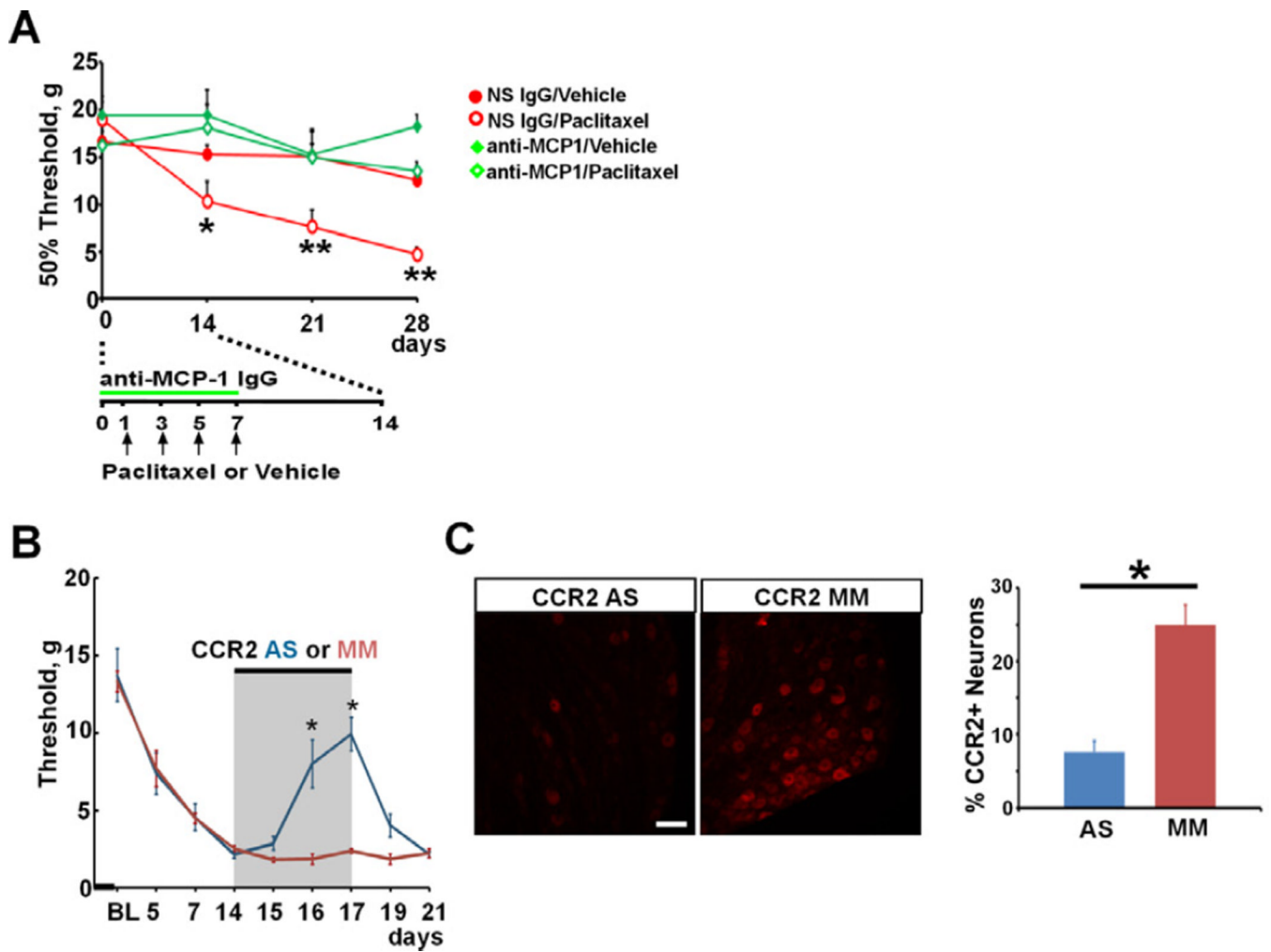


**Figure 6.** Blockade of MCP-1 or CCR2 attenuates paclitaxel-induced mechanical hypersensitivity. **A.** Intrathecal anti-MCP-1 IgG prevents paclitaxel-induced mechanical hypersensitivity ( $n = 7, 7, 5$  and  $6$  for non-specific (NS) IgG/vehicle, NS IgG/paclitaxel, anti-MCP-1/vehicle and anti-MCP-1/paclitaxel, respectively). \*  $p < 0.05$ , \*\*  $p < 0.01$ , two-way ANOVA. **B.** Intrathecal CCR2 antisense (AS) but not mismatch (MM) ODN significantly reduces paclitaxel-induced mechanical hypersensitivity. \*  $p < 0.01$ , one-way ANOVA. BL: baseline. **C.** Intrathecal CCR2 AS but not MM ODN significantly reduces the induction of CCR2 in DRG from paclitaxel-treated animals. Tissues are collected on the last day of CCR2 ODNsb treatment (Day 17 following chemotherapy). \*  $p < 0.01$ ,  $n = 3$  each group,  $t$ -test. Scale bar:  $100 \mu\text{m}$ .

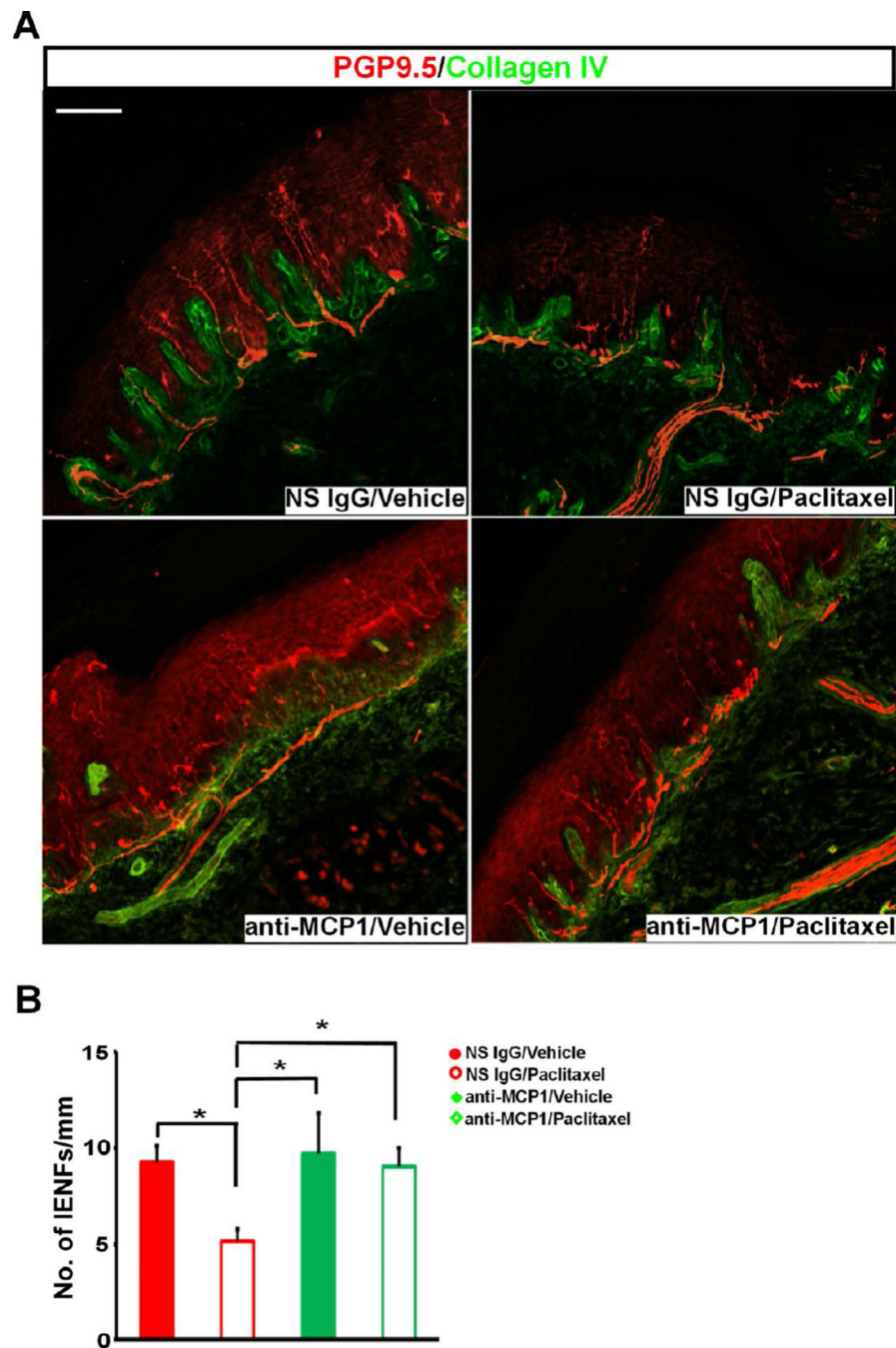


**Figure 7.** Blockade MCP-1 prevents the loss of IENFs induced by paclitaxel. **A.** Representative images of IENFs in glabrous skin of hindpaw foot pad. The density of IENFs stained by PGP9.5 (red) crossing dermal/epidermal border (green) is much lower in NS IgG/paclitaxel group and intrathecal anti-MCP-1 IgG prevents the loss of IENFs. Confocal images are taken with Z-stack of 2 $\mu$ m-step in one view using 20X objective and montaged as a single image. **B.** Paclitaxel induces a significant decrease in the density of IENFs and anti-MCP-1 treatment prevents the loss of IENFs (n = 6, 7, 4 and 4 for NS IgG/vehicle, NS IgG/



paclitaxel, anti-MCP-1/vehicle and anti-MCP-1/paclitaxel, respectively). \*  $p < 0.05$ , one-way ANOVA. Scale bar: 100  $\mu\text{m}$ .

